

## Structure determination at room temperature and phase transition studies above $T_c$ in $ABi_4Ti_4O_{15}$ (A = Ba, Sr or Pb)

G NALINI and T N GURU ROW\*

Solid State and Structural Chemistry Unit, Indian Institute of Science, Bangalore 560 012, India

MS received 9 May 2002

**Abstract.** The room temperature structure of three compounds belonging to the Aurivillius family ( $n = 4$ ),  $ABi_4Ti_4O_{15}$  (A = Ba, Sr or Pb) has been analysed.  $BaBi_4Ti_4O_{15}$  crystallizes in a tetragonal  $I4/mmm$  space group whereas  $SrBi_4Ti_4O_{15}$  and  $PbBi_4Ti_4O_{15}$  crystallize in the orthorhombic space group  $A2_1am$ . The starting model for the Sr and Pb analogues was derived from *ab initio* methods and refined using the Rietveld method. The cations Ba and Sr are disordered over the Bi sites while the Pb cation is found exclusively in the  $[Bi_2O_2]^{2+}$  layers. The  $TiO_6$  octahedra are tilted with the Ti–O bonds forming zigzag chains along the ‘c’ axis. The displacement of Bi atoms along the ‘a’ axis might be responsible for ferroelectricity in these compounds. The high temperature X-ray data above  $T_c$  indicate no structural transition for A = Ba and Pb while A = Sr transforms to the tetragonal structure.

**Keywords.** *ab initio* structure; powder XRD; Rietveld refinement; Aurivillius phases.

### 1. Introduction

For the past decade, there has been considerable interest in layered oxides exhibiting ferroelectric, piezoelectric and other related properties due to their wide ranging application in technical devices (Park *et al* 1999). One such family of oxides is the Aurivillius type of oxides with the general formula  $[Bi_2O_2][A_{n-1}B_nO_{3n+3}]$  ( $n = 1, 2, 3, 4$ ), where the  $[Bi_2O_2]^{2+}$  layers are interleaved with  $n$  perovskite-type layers having the composition (Subbarao 1962)  $[A_{n-1}B_nO_{3n+1}]$ .  $ABi_4Ti_4O_{15}$  (A = Ba, Sr and Pb) are members of the  $n = 4$  series of this Aurivillius family. It can be inferred from Raman studies that these compounds exhibit a ferroelectric–paraelectric phase transition at elevated temperature (Kojima *et al* 1995).

Extensive crystal structure analyses have been carried out for the  $n = 2$  layered Aurivillius oxides by powder X-ray and neutron diffraction techniques (Ismunandar and Kennedy 1996, 1999). The results of these studies have identified disorder in the A-type cation over the perovskite and the  $Bi_2O_2$  layers. From the data available previously (Kojima *et al* 1995) for  $n = 4$ , assumptions have been made concerning the evolution of these phases from ferroelectric to paraelectric regimes. More over all these compounds are expected to crystallize in the tetragonal system, space group ( $I4/mmm$ ) which is the idealized parent structure for all the Aurivillius family of compounds (Subbarao 1962) above  $T_c$ . Aurivillius (1950) has reported a model for  $BaBi_4Ti_4O_{15}$  at room tempe-

rate, which has a tetragonal symmetry ( $I4/mmm$  space group). In case of the A = Sr, Pb structures, an orthorhombic symmetry with the space group  $A2_1am$  was reported earlier (JCPDS-Card Nos: 43-0972 and 43-0973 1997). Recently, a detailed neutron diffraction study (Hervoches *et al* 2002) was also reported for  $SrBi_4Ti_4O_{15}$ . In the following sections, we report the room temperature structural features of all three compounds determined using high-resolution powder X-ray diffraction data. The starting model for A = Ba compound was derived from the earlier report and refined via the Rietveld (1969) method. The starting models for A = Sr, Pb analogues were derived from *ab initio* (Altomare *et al* 1994, 1995) methods and the model refined to completion by the Rietveld (1969) method. X-ray diffraction data for all the three compounds at elevated temperature (above  $T_c$ ) have been collected and an evaluation of their structures is also presented.

### 2. Experimental

$ABi_4Ti_4O_{15}$  (A = Ba, Sr or Pb) were synthesized by the solid-state reaction of  $ACO_3$  (A = Ba, Sr or Pb),  $Bi_2O_3$  and  $TiO_2$  at 1223 K for 15 h, then at 1323 K for 15 h with intermittent grinding after each heating step. Quantitative elemental analyses on all samples were carried out on a JEOL JSM-840 EDAX machine in order to confirm the exact composition of the metal ions. The ratio of the metal ions thus calculated (table 1) from the EDAX measurements correspond to that of the ions taken initially for syntheses. Preliminary X-ray diffraction data

\*Author for correspondence

revealed that the compounds were formed without any impurity phases.

High-resolution room temperature X-ray diffraction data on all the three compounds were collected on a STOE/STADI-P X-ray powder diffractometer with Germanium monochromated  $\text{CuK}\alpha_1$  ( $\lambda = 1.54056 \text{ \AA}$ ) radiation in the transmission mode. The samples were rotated during data collection to reduce orientation effects, if any and the data were recorded using a linear PSD. The X-ray data were measured in the range  $2\theta = 3$  to  $89.80^\circ$  at steps of  $0.02^\circ$  with exposure time of 6 s per step.

The powder diffraction data at elevated temperatures were collected in the Debye-Scherrer mode. The compounds were filled in a quartz capillary of 0.3 mm diameter and rotated during the data collection with a uniform speed in the furnace. The reported  $T_c$  for the compounds for A = Ba, Sr and Pb are 703 K, 803 K and 843 K, respectively (Takashige *et al* 1995). The temperature of the furnace was maintained at  $723 \pm 5 \text{ K}$ ,  $873 \pm 7 \text{ K}$  and  $873 \pm 5 \text{ K}$  during the data collection for A = Ba, Sr and Pb, respectively which ensures the temperatures to be above  $T_c$ . The data were recorded using a curved PSD in three overlapping ranges with the overall  $2\theta = 3^\circ$  to  $80^\circ$  in steps of  $0.03^\circ$  with 30 min exposure time per range.

### 3. Structure determination and refinement

#### 3.1 Room temperature data

The trial and error indexing program TREOR (Werner 1964) was used to determine the unit cell parameters. The indexing for all the lines for  $\text{BaBi}_4\text{Ti}_4\text{O}_{15}$  were checked and confirmed with the JCPDS card no 35-0757. The atomic coordinates were taken from the initial report by Aurivillius and the structure was refined to completion. The GSAS package (Larson and von Dreele 1987) was employed for the Rietveld refinements in this case.

The compounds,  $\text{SrBi}_4\text{Ti}_4\text{O}_{15}$  and  $\text{PbBi}_4\text{Ti}_4\text{O}_{15}$ , belong to the orthorhombic system and the derived cell parameters match with those in JCPDS card numbers 43-0973 and 43-0972. The full pattern fitting and peak decomposition in the space group  $A2_1am$  were carried out using the program EXTRA (Altomare *et al* 1994) resulting in 124 independent reflections, respectively. The pattern

fitting was also performed with other possible space groups like  $Pna2_1$  and  $Fmm2$  to ensure the correctness in the assignment of the space group. SIRPOW92 (Altomare *et al* 1994) was then used to locate the positional parameters of strontium/lead, bismuth and titanium atoms, which formed the starting model for preliminary Rietveld refinement using the GSAS program. Subsequent difference-Fourier maps revealed the positions of the remaining (oxygen) atoms, which were incorporated in further refinements.

The profiles were fitted using a pseudo-Voigt function. The Chebyshev polynomial consisting of 3–7 coefficients was used to define the background. In all three compounds, it was assumed initially that the cations are fully ordered with the Sr, Ba or Pb atoms occupying the A sites only (50 : 50). The heavy atoms were then refined with the occupancy and the thermal parameters fixed. The positional parameters of the oxygen atoms were also refined.

Further, the thermal parameters of the heavy atoms were refined alternately with the occupancies. It was observed that the occupancy values of the Bi atom at  $[\text{Bi}_2\text{O}_2]^{2+}$  layer and the Ba/Sr/Pb atoms in the A sites refine to lower values suggesting a disorder. The atoms Ba/Sr/Pb were proposed to be distributed both at A sites as well as at the  $[\text{Bi}_2\text{O}_2]^{2+}$  layer to account for this disorder and the overall stoichiometry was maintained using the occupancy constraint. It should be noted that while in the present study the Sr atoms in  $\text{SrBi}_4\text{Ti}_4\text{O}_{15}$  are clearly distributed in both the A sites and the  $[\text{Bi}_2\text{O}_2]^{2+}$  layer, the neutron diffraction report indicates that the Sr atoms are restrained to A sites only (Hervoches *et al* 2002). However, it must be pointed out that the scattering power of Bi and Sr atoms are widely different in X-ray diffraction

**Table 1.** Results of EDAX analyses for  $\text{ABi}_4\text{Ti}_4\text{O}_{15}$ .

Initial mixtures (Bi : A)	Powder samples (Bi : A)
80 : 20	77.3 : 22.7
80 : 20	78 : 18
80 : 20	77 : 21

Relative concentration of A; A = Ba, Sr or Pb (%).

**Table 2.** Crystal data for  $\text{ABi}_4\text{Ti}_4\text{O}_{15}$  (A = Ba, Sr or Pb) at 298 K.

Formula	$\text{BaBi}_4\text{Ti}_4\text{O}_{15}$	$\text{SrBi}_4\text{Ti}_4\text{O}_{15}$	$\text{PbBi}_4\text{Ti}_4\text{O}_{15}$
Formula weight	1404.85	1355.13	1474.70
Colour	Yellow	Yellow	Yellow
Space group	$I4/mmm$	$A2_1am$	$A2_1am$
Z	2	4	4
$\lambda$ ( $\text{\AA}$ )	1.54056	1.54056	1.54056
$2\theta$	3–89.80°	3–89.80°	3–89.80°
Number of reflections	30	29	29
Number of structural parameters	17	51	51
$a$ ( $\text{\AA}$ )	3.8640(1)	5.4510(5)	5.4267(1)
$b$ ( $\text{\AA}$ )		5.4415(5)	5.4458(1)
$c$ ( $\text{\AA}$ )	41.8341(14)	41.0233(13)	41.4121(12)
$V$ ( $\text{\AA}^3$ )	622.84(4)	1217.12(8)	1223.86(8)
$R_{wp}$	7.28%	7.5%	9.87%
$R_p$	5.47%	5.72%	6.66%
$R$ ( $I, hkl$ )	10.44%	9.03%	8.72%
Number of data points	4349	4349	4349

**Table 3a.** Final atomic coordinates from powder X-ray data at 298 K for BaBi<sub>4</sub>Ti<sub>4</sub>O<sub>15</sub>.

Atom	Site	x	y	z	Occupancy	$U_{\text{iso}}(\text{\AA}^2)$
Bi(1)	2e	0.000	0.000	0.0000	0.89(1)	0.0275(13)
Ba(1)	2e	0.000	0.000	0.0000	0.11(1)	0.0275(13)
Bi(2)	4e	0.000	0.000	0.1055(1)	0.83(1)	0.0337(10)
Ba(2)	4e	0.000	0.000	0.1055(1)	0.17(1)	0.0337(10)
Bi(3)	4e	0.000	0.000	0.2198(1)	0.77(2)	0.0196(10)
Ba(3)	4e	0.000	0.000	0.2198(1)	0.23(2)	0.0196(10)
Ti(1)	4e	0.000	0.000	0.4491(2)	1.000	0.0029(14)
Ti(2)	4e	0.000	0.000	0.3452(2)	1.000	0.0029(14)
O(1)	2b	0.000	0.000	0.5000	1.000	0.0288(27)
O(2)	8g	0.000	0.500	0.0446(3)	1.000	0.0288(27)
O(3)	4e	0.000	0.000	0.4086(6)	1.000	0.0288(27)
O(4)	8g	0.000	0.500	0.1430(4)	1.000	0.0288(27)
O(5)	4e	0.000	0.000	0.3116(6)	1.000	0.0288(27)
O(6)	4d	0.000	0.500	0.2500	1.000	0.0288(27)

$U_{\text{iso}}$  is the isotropic thermal parameter.

**Table 3b.** Final atomic coordinates from powder X-ray data at 298 K for SrBi<sub>4</sub>Ti<sub>4</sub>O<sub>15</sub>.

Atom	Site	x	y	z	Occupancy	$U_{\text{iso}}(\text{\AA}^2)$
Bi(1)	8b	1.0361(26)	0.2547(17)	0.1054(1)	0.74(1)	0.0265(9)
Sr(1)	8b	1.0361(26)	0.2547(17)	0.1054(1)	0.26(1)	0.0265(9)
Bi(2)	4a	0.0404(55)	0.2412(30)	0.0000	0.89(1)	0.0226(7)
Sr(2)	4a	0.0404(55)	0.2412(30)	0.0000	0.11(1)	0.0226(7)
Bi(3)	8b	0.0402(45)	0.2412(18)	0.2187(18)	0.72(1)	0.0188(11)
Sr(3)	8b	0.0402(45)	0.2412(18)	0.2187(18)	0.28(1)	0.0188(11)
Ti(1)	8b	0.034(11)	0.752(10)	0.1556(2)	1.00	0.0095(13)
Ti(2)	8b	0.032(13)	0.757(15)	0.0494(2)	1.00	0.0095(13)
O(1)	4a	0.065(21)	0.697(12)	0.0939(5)	1.00	0.0129(27)
O(2)	8b	0.3112(22)	-0.005(50)	0.2514(31)	1.00	0.0129(27)
O(3)	8b	0.088(32)	0.819(25)	0.0000	1.00	0.0129(27)
O(4)	8b	0.366(35)	0.922(35)	0.0533(13)	1.00	0.0129(27)
O(5)	8b	0.308(25)	-0.005(28)	0.1443(7)	1.00	0.0129(27)
O(6)	8b	0.297(36)	0.510(45)	0.0451(9)	1.00	0.0129(27)
O(7)	8b	0.277(25)	0.510(44)	0.1428(7)	1.00	0.0129(27)
O(8)	8b	0.036(26)	0.772(15)	0.1923(5)	1.00	0.0129(27)

$U_{\text{iso}}$  is the isotropic thermal parameter.

**Table 3c.** Final atomic coordinates from powder X-ray data at 298 K for PbBi<sub>4</sub>Ti<sub>4</sub>O<sub>15</sub>.

Atom	Site	x	y	z	Occupancy	$U_{\text{iso}}(\text{\AA}^2)$
Bi(1)	8b	1.0542(16)	0.2403(11)	0.1055(1)	1.00	0.0198(8)
Bi(2)	4a	0.0484(27)	0.2555(23)	0	1.00	0.0158(8)
Bi(3)	8b	0.0363(16)	0.2592(15)	0.2192(1)	0.52(2)	0.0258(119)
Pb(3)	8b	0.0363(16)	0.2592(15)	0.2192(1)	0.48(2)	0.0258(119)
Ti(1)	8b	0.037(85)	0.7418(54)	0.1553(2)	1.00	0.0090(15)
Ti(2)	8b	0.645(47)	0.7689(61)	0.0498(2)	1.00	0.0090(15)
O(1)	8b	-0.001(40)	0.6817(99)	0.9360(6)	1.00	0.0179(27)
O(2)	8b	0.282(35)	0.092(37)	0.2451(1)	1.00	0.0179(27)
O(3)	4a	0.000(31)	0.808(15)	0	1.00	0.0179(27)
O(4)	8b	0.379(12)	0.902(12)	0.045(10)	1.00	0.0179(27)
O(5)	8b	0.288(17)	0.046(12)	0.1472(8)	1.00	0.0179(27)
O(6)	8b	0.309(20)	0.465(16)	0.044(7)	1.00	0.0179(27)
O(7)	8b	0.310(20)	0.465(16)	0.1432(8)	1.00	0.0179(27)
O(8)	8b	0.052(20)	0.737(22)	0.1942(6)	1.00	0.0179(27)

$U_{\text{iso}}$  is the isotropic thermal parameter.

unlike in neutron diffraction and hence our observations are more reliable. Also, the isotropic thermal parameters of all the oxygen atoms were constrained together and refined. The details of the crystal data and refinements are given in tables 2, 3a, 3b and 3c, respectively. The observed, difference and calculated patterns of all the three compounds are shown in figures 1, 2 and 3, respectively. Selected bond distances are listed in table 4.

### 3.2 High temperature data

The high temperature powder patterns of the three compounds recorded at  $723 \pm 5$  K,  $873 \pm 7$  K and  $873 \pm 5$  K, respectively are shown in figures 4–6.  $\text{BaBi}_4\text{Ti}_4\text{O}_{15}$  and  $\text{PbBi}_4\text{Ti}_4\text{O}_{15}$  do not show any structural phase transition whereas  $\text{SrBi}_4\text{Ti}_4\text{O}_{15}$  shows a structural phase transition. The lattice parameters for this pattern (figure 5) were determined and refined using the program Appleman (Sonneveld and Visser 1975) from the suite of programs,

**Table 4.** Ti–O bond distances (Å) in  $\text{ABi}_4\text{Ti}_4\text{O}_{15}$  (A = Ba, Sr or Pb).

(Ti–O) Octahedra	$\text{BaBi}_4\text{Ti}_4\text{O}_{15}$	$\text{SrBi}_4\text{Ti}_4\text{O}_{15}$	$\text{PbBi}_4\text{Ti}_4\text{O}_{15}$
Ti(1)–O(1)/O(1)/O(1)	1.690(1)	2.079(4)	1.744(2)
Ti(1)–O(3)/O(7)/O(7)	2.129(1)	1.983(3)	2.609(12)
Ti(1)–O(2)/O(5)/O(5)	1.950(1)	1.906(2)	1.806(1)
Ti(1)–O(2)/O(8)/O(8)	1.952(2)	1.516(4)	1.626(4)
Ti(1)–O(2)/O(7)/O(7)	1.950(1)	1.943(4)	2.175(2)
Ti(1)–O(2)/O(5)/O(5)	1.952(1)	2.053(2)	2.177(1)
Ti(2)–O(5)/O(6)/O(6)	1.993(1)	1.951(3)	2.018(1)
Ti(2)–O(4)/O(3)/O(3)	1.996(1)	2.084(2)	2.110(4)
Ti(2)–O(4)/O(6)/O(6)	1.993(1)	1.986(4)	2.012(1)
Ti(2)–O(4)/O(3)/O(3)	1.996(2)	2.036(2)	1.868(5)
Ti(2)–O(4)/O(1)/O(1)	1.401(1)	1.864(1)	2.066(1)
Ti(2)–O(3)/O(4)/O(4)	2.657(1)	2.557(3)	2.066(1)

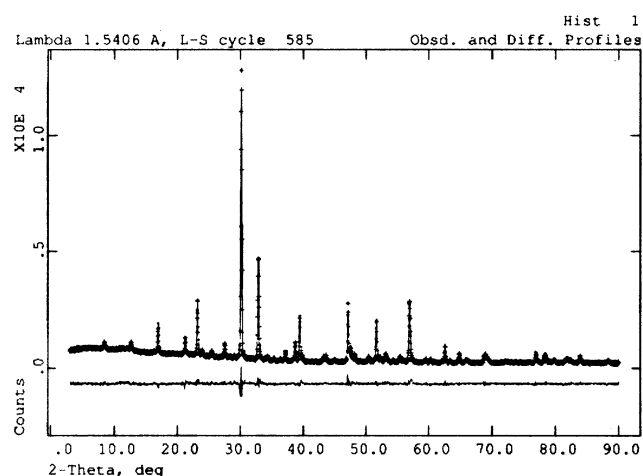


**Figure 1.** Observed, calculated and difference patterns of  $\text{BaBi}_4\text{Ti}_4\text{O}_{15}$ .

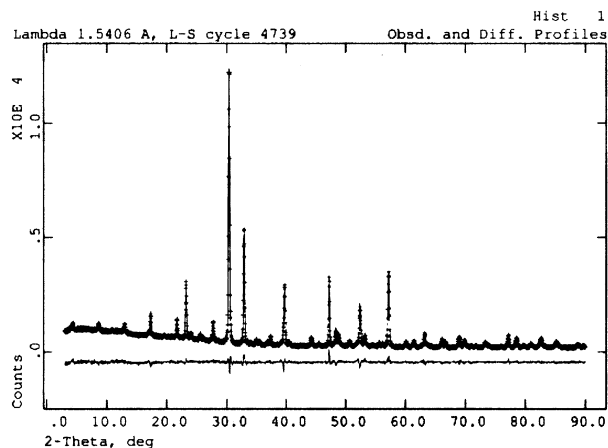


**Figure 2.** Observed, calculated and difference patterns of  $\text{SrBi}_4\text{Ti}_4\text{O}_{15}$ .

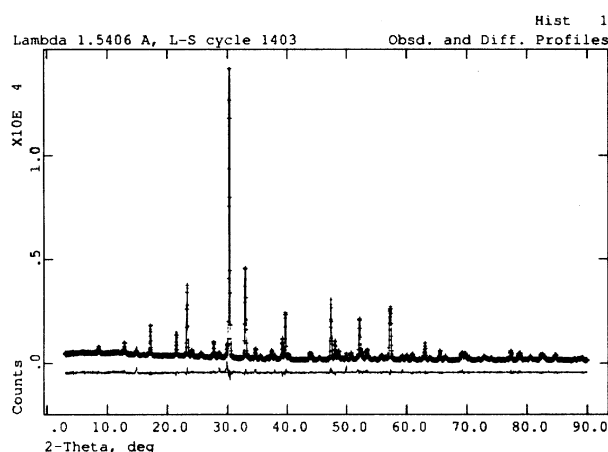


**Figure 3.** Observed, calculated and difference patterns of  $\text{PbBi}_4\text{Ti}_4\text{O}_{15}$ .

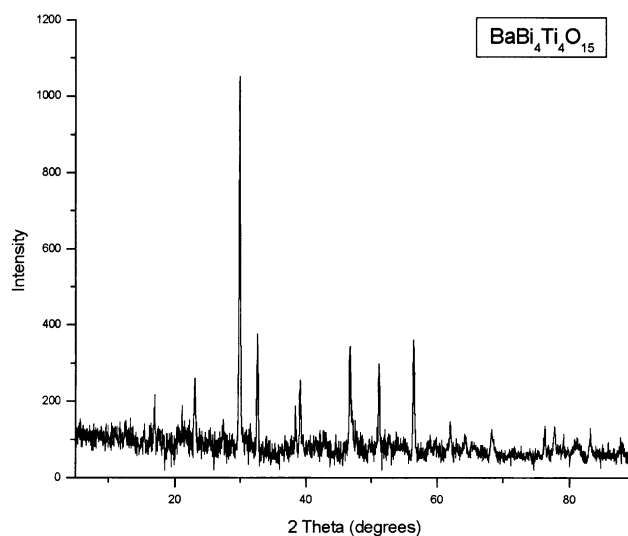


**Figure 4.** High temperature powder X-ray diffraction pattern of  $\text{BaBi}_4\text{Ti}_4\text{O}_{15}$ .

Proszki (Sonneveld and Visser 1975). It is observed that this high temperature phase transforms to the prototype tetragonal system ( $I4/mmm$ ).

## 4. Results and discussion

### 4.1 Room temperature data

The crystal structure of  $ABi_4Ti_4O_{15}$  ( $A = Ba, Sr$  or  $Pb$ ) is as shown in figure 7. The titanium occupies the  $MO_6$  position in the perovskite layer. However, the continuous O–Ti–O chains expected in a simple perovskite is disrupted at every  $n = 4$  along the  $c$  axis by  $[Bi_2O_2]^{2+}$  layers. The Ti–O distances range from 1.401(4) to 2.657(1) Å with alternate bonds being long and short to result in a zigzag arrangement of  $TiO_6$  octahedra (Frit and Mercurio 1992) (table 4). The range of the Ti–O distances calcu-

lated appear to be rather large than those reported in the literature for similar systems. However, more accurate bond lengths have been obtained via neutron diffraction studies for  $SrBi_4Ti_4O_{15}$  (Hervoches *et al* 2002). The differences in ionic radii of Ba, Sr and Pb ions also appear to influence the tilt and distortion of the  $TiO_6$  octahedra. The Bi–O distances range from 2.25(1) Å to 3.31(3) Å.

The structure of  $BaBi_4Ti_4O_{15}$  has three Bi atoms in the asymmetric unit with one of the atoms [Bi(3)] forming the  $[Bi_2O_2]^{2+}$  layer, while the other two [Bi(1) and Bi(2)] belong to the perovskite layers. Bi(1) and Bi(2) are

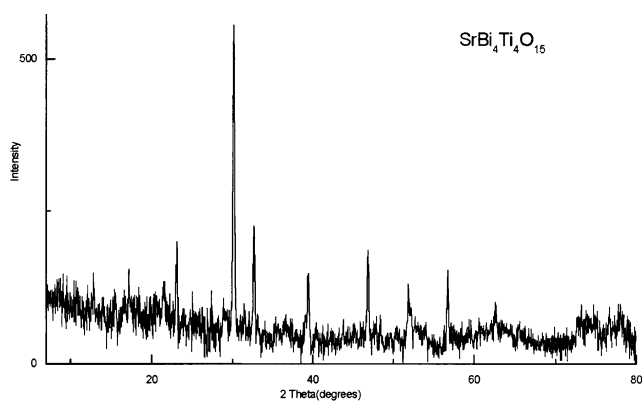


**Figure 5.** High temperature powder X-ray diffraction pattern of  $SrBi_4Ti_4O_{15}$ .

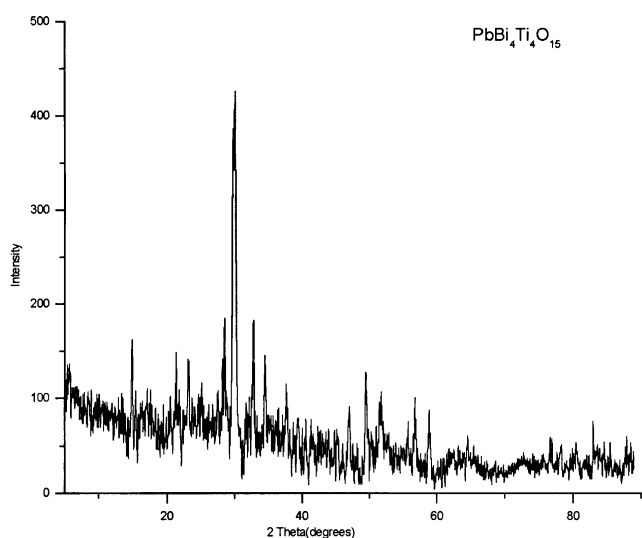


**Figure 6.** High temperature powder X-ray diffraction pattern of  $PbBi_4Ti_4O_{15}$ .

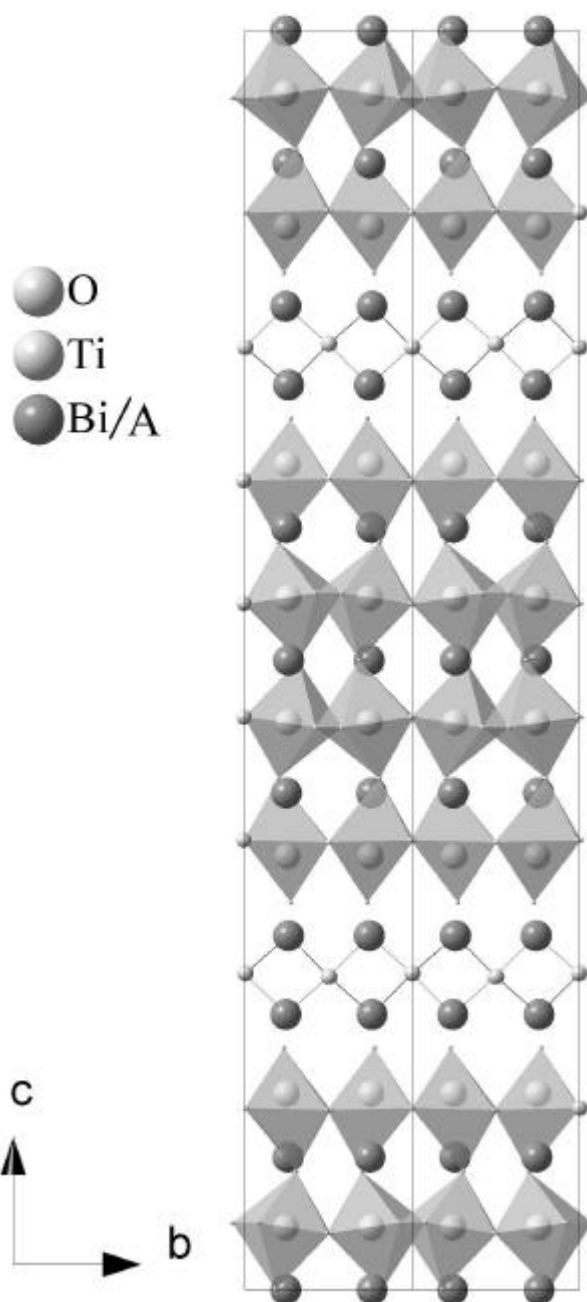


**Figure 7.** Alternating perovskite and bismuth oxide layers viewed down the 'a' axis of  $ABi_4Ti_4O_{15}$ .

**Table 5.** Selected bond valence sums (Å) in  $\text{ABi}_4\text{Ti}_4\text{O}_{15}$  (A = Ba, Sr or Pb).

	Bi(1) and Bi(2)	Bi(3)
$\text{BaBi}_4\text{Ti}_4\text{O}_{15}$		
Ordered*	2.414	2.62
Disordered <sup>+</sup>	3.08	2.72
$\text{SrBi}_4\text{Ti}_4\text{O}_{15}$		
Ordered*	2.66	2.71
Disordered <sup>+</sup>	2.70	2.76
$\text{PbBi}_4\text{Ti}_4\text{O}_{15}$		
Ordered*	2.87	2.86
Disordered <sup>+</sup>	2.71	2.78

\*Indicates only the Bi atoms in the A site and the  $[\text{Bi}_2\text{O}_2]^{2+}$  site; <sup>+</sup>indicates the distribution of A cations in both A site and the  $[\text{Bi}_2\text{O}_2]^{2+}$  site and the VBS is calculated by considering the contribution from both the Bi and A atoms : : mean bond valence sum = (bond valence sum of Bi1 + bond valence sum of A)/2; A = Ba/Sr/Pb.

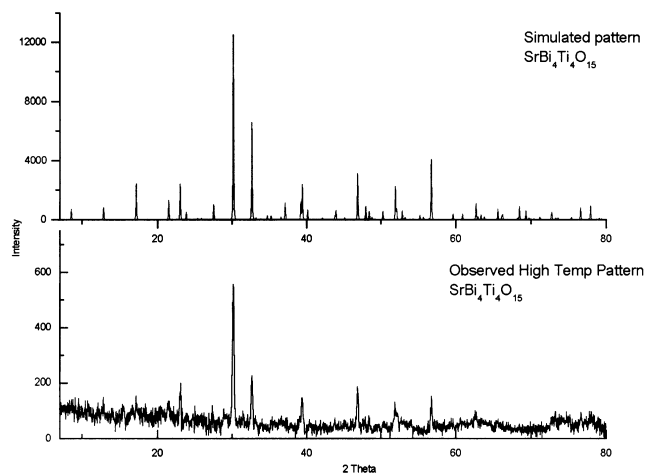
coordinated to 12 oxygen atoms and Bi(3) is coordinated to 8 oxygens. The structure of  $\text{BaBi}_4\text{Ti}_4\text{O}_{15}$  is refined using the Rietveld method in the space group  $I4/mmm$ . However, it is noteworthy that earlier reports (Harnagea *et al* 1999; Satyalakshmi *et al* 1999) on thin films of this material demonstrate that it is ferroelectric when grown in specified directions. This suggests the possibility of non-centrosymmetric arrangements in specific domains in certain crystallographic directions.

The room temperature structures of  $\text{SrBi}_4\text{Ti}_4\text{O}_{15}$  and  $\text{PbBi}_4\text{Ti}_4\text{O}_{15}$  depict a coordination environment similar to that in  $\text{BaBi}_4\text{Ti}_4\text{O}_{15}$  except at Bi(1) which is 10 coordinated in  $\text{SrBi}_4\text{Ti}_4\text{O}_{15}$  and 11 coordinated in  $\text{PbBi}_4\text{Ti}_4\text{O}_{15}$ . Ferroelectric studies on these ceramics revealed that domain reorientation occur almost exclusively on the *ab*-plane of the orthorhombic cell (Thomazini and Eiras 1999). This is consistent with observed shift of Bi atoms along *a* and *b* directions.

The occupancy refinements suggest that only in case of  $\text{PbBi}_4\text{Ti}_4\text{O}_{15}$  the Pb cations get localized in the  $\text{Bi}_2\text{O}_2$  layers. However, it is hard to ascertain this feature since the scattering factors for X-rays for Bi and Pb are nearly the same. On the other hand, it is clear that in the other two compounds the Ba/Sr cations are distributed in both  $\text{Bi}_2\text{O}_2$  and the perovskite layers. Table 5 provides a list of valence bond sums (Brown and Altermatt 1985) (VBS) in all these three structures, which indicate a measure of the extent of disorder in these phases. It also compares the tendency of the three oxides to incorporate A type cations in the  $[\text{Bi}_2\text{O}_2]$  layer and the perovskite layers.

#### 4.2 High temperature data

The high temperature structure of  $\text{BaBi}_4\text{Ti}_4\text{O}_{15}$  above  $T_c$  (723 K) does not show any significant deviations in the

**Figure 8.** Comparison of the observed and simulated patterns for the high temperature phase of  $\text{SrBi}_4\text{Ti}_4\text{O}_{15}$ .

X-ray diffraction pattern thereby indicating no structural phase transition. The  $\text{PbBi}_4\text{Ti}_4\text{O}_{15}$  likewise shows no structural phase transition above  $T_c$  (843 K). A change in the X-ray diffraction pattern is observed in the case of  $\text{SrBi}_4\text{Ti}_4\text{O}_{15}$  above  $T_c = 803$  K (data collected at 873 K). On careful examination followed by indexing the pattern it is observed that the crystal system transforms to a tetragonal  $I4/mmm$  symmetry with  $a = 3.8745(18)$  Å and  $c = 41.310(24)$  Å. Figure 8 shows a comparison of the simulated pattern based on a possible model for  $\text{SrBi}_4\text{Ti}_4\text{O}_{15}$  derived from the room temperature structure of  $\text{BaBi}_4\text{Ti}_4\text{O}_{15}$  with the observed diffraction pattern. Further, attempts to refine the observed diffraction pattern were not made due to the lack of quality data at such high temperatures. However, the report (Hervoches *et al* 2002) on the high temperature neutron diffraction on  $\text{SrBi}_4\text{Ti}_4\text{O}_{15}$  verifies this model unequivocally.

## 5. Conclusions

In summary, it may be stated that the room temperature crystal structures of three  $n = 4$  Aurivillius type of oxides have been refined from high resolution X-ray diffraction data. The pattern decomposition and peak extraction methods have been used for the first time to derive starting models for  $\text{SrBi}_4\text{Ti}_4\text{O}_{14}$  and  $\text{PbBi}_4\text{Ti}_4\text{O}_{15}$ . A model has been proposed for this high temperature phase. It is also confirmed that the ferroelectric to paraelectric phase transition in  $\text{BaBi}_4\text{Ti}_4\text{O}_{15}$  and  $\text{PbBi}_4\text{Ti}_4\text{O}_{15}$  is not accompanied by a structural phase transition. The zigzag arrangement of the distorted  $\text{TiO}_6$  octahedra as observed in the  $n = 2$  series of Aurivillius phases are found in these structures as well. A rational explanation for the distribution of the Ba/Sr/Pb cations in the A sites as well as the  $[\text{Bi}_2\text{O}_2]^{2+}$  sites is provided based on the VBS calculations.  $\text{SrBi}_4\text{Ti}_4\text{O}_{15}$  shows a structural transition to the

prototype tetragonal structure in the space group  $I4/mmm$  at 803 K. A model has been proposed for this high temperature phase. It is also confirmed that the ferroelectric to paraelectric phase transition in  $BaBi_4Ti_4O_{15}$  and  $PbBi_4Ti_4O_{15}$  is not accompanied by a structural phase transition.

## References

- Altomare A, Burla M C, Cascarano G, Giacovazzo C, Guagliardi A and Moliterni A G G 1994 *J. Appl. Crystallogr.* **27** 35
- Altomare A, Burla M C, Cascarano G, Giacovazzo C, Guagliardi A and Moliterni A G G 1995 *J. Appl. Crystallogr.* **28** 842
- Aurivillius B 1950 *ARKEA foer Kemi* **2** 19
- Brown I D and Alternatt D 1985 *Acta Crystallogr.* **B41** 244
- Frit B and Mercurio J P 1992 *J. Alloys & Compounds* **188** 27
- Harnagea C, Pignolet A, Alexe M, Satyalakshmi K M, Hesse D and Gosele U 1999 *Jpn J. Appl. Phys.* **38** 1255
- Hervoches C H and Lightfoot Philip 1999 *Chem. Mater.* **11** 3359
- Hervoches C H, Snedden A, Richard R, Kilcoyne S H, Manuel P and Lightfoot P 2002 *J. Solid State Chem.* **164** 280
- Ismunandar and Kennedy B J 1996 *J. Solid State Chem.* **126** 135
- Ismunandar and Kennedy B J 1999 *J. Mater. Chem.* **9** 541
- JCPDS-Card Nos: 43-0972 & 43-0973 1997 (International Centre for Diffraction Data)
- Kojima S, Imaizumi R, Hamazaki S and Takashige M 1995 *J. Mol. Struc.* **348** 37
- Larson A C and von Dreele R B 1987 Los Alamos Laboratory Report No. LA-UR 86-748
- Park H B, Kang B S, Bu S D, Noh T W, Lee J and Jo W 1999 *Nature* **401** 682
- Rietveld H M 1969 *J. Appl. Crystallogr.* **2** 65
- Satyalakshmi K M, Alexe M, Pignolet A, Zakharov N D, Harnagea C, Senz S and Hesse D 1999 *Appl. Phys. Lett.* **74** 603
- Sonneveld E J and Visser J W 1975 *J. Appl. Crystallogr.* **8** 1
- Subbarao E C 1962 *J. Am. Ceram. Soc.* **45** 166
- Thomazini D and Eiras J A 1999 *J. Am. Ceram. Soc.* **82** 2368
- Werner P 1964 *Z. Krist.* **120** 385